Journal of Solid State Chemistry 190 (2012) 186–190

Contents lists available at SciVerse ScienceDirect

Journal of Solid State Chemistry

journal homepage: www.elsevier.com/locate/jssc

Influence of structural distortions upon photoluminescence properties of Eu^{3+} and Tb^{3+} activated $Na_3Ln(BO_3)_2$ (Ln=Y, Gd) borates

S. Asiri Naidu [a], S. Boudin [a,*], U.V. Varadaraju [b], B. Raveau [a]

[a] Laboratoire CRISMAT (CNRS UMR6508), ENSICAEN, Université de Caen, 6 Bd Maréchal Juin, 14050 Caen Cedex, France
[b] Department of Chemistry, Indian Institute of Technology Madras, Chennai 600036, India

ARTICLE INFO

Article history:
Received 14 November 2011
Received in revised form
14 February 2012
Accepted 16 February 2012
Available online 27 February 2012

Keywords:
Europium and terbium doped borates
Yttrium and gadolinium borates
photoluminescence
Energy transfer
Critical concentration

ABSTRACT

The comparative study of the structure and photoluminescence (PL) properties of the Eu^{3+} and Tb^{3+} activated $Na_3Ln(BO_3)_2$, with Ln=Y, Gd, showed the important role of the host lattice structure upon PL. Higher emission intensities of Eu^{3+} and Tb^{3+} are observed for $Na_3Gd(BO_3)_2$ than for $Na_3Y(BO_3)_2$, through direct Eu^{3+} excitation at 395 nm for Eu^{3+} doped borates, and through Gd^{3+} excitation around 280 nm for Tb^{3+} doped borates. This higher performance for $Na_3Gd(BO_3)_2$ is due to the less regular environment of Eu^{3+} (Tb^{3+}) in the Gd sites than in the Y sites and to energy transfer from Gd^{3+} to Eu^{3+}(Tb^{3+}). The smaller critical concentration in $Na_3Ln_{1-x}Tb_x(BO_3)_2$ observed for Ln=Gd, x=0.5, compared to x=0.6 for Ln=Y, is explained by shorter Ln–Ln distances (4.11 Å for Gd–Gd vs. 4.59 Å for Y–Y). Both $Na_3Y_{0.4}Tb_{0.6}(BO_3)_2$ and $Na_3Gd_{0.5}Tb_{0.5}(BO_3)_2$ show intense green emission under UV excitation.

1. Introduction

Rare-earth-based oxides are extensively studied for their PL properties, due to the fact that the Ln^{3+} cations exhibit a large range of emission colors, based on 4f–4f or 5d–4f transitions [1]. In this respect rare earth borates are promising candidates for solid state lighting applications, especially when they are doped with Eu^{3+} and Tb^{3+} ions which are excellent red and green emitters, respectively. This is the case of phosphors (Y,Gd)BO_3:Eu^{3+}, YBO_3:Tb^{3+}, $Na_2Y_2B_2O_7$:Eu^{3+} and $Na_2Gd_2B_2O_7$:Eu^{3+} [2–7]. Moreover, the Ln^{3+} cations may play the role of activator, as shown for the Gd^{3+} phosphors Gd_2BaZnO_5:Eu^{3+}, $BaGdB_9O_{16}$:Eu^{3+} and $Ca_6Gd_2Na_2(PO_4)_6F_2$:Eu^{3+} [8–10]. But besides the presence of sensitizer ions or activators, the PL properties of the materials also depend on the nature of the host lattice, especially on the local geometry of the Ln^{3+} sites, and on the possible interactions between the Ln^{3+} cations in the structure such as the Ln^{3+}–Ln^{3+} distances. Thus, it appears of capital importance to try to establish correlations between the crystal structure of the host lattices and the PL properties of the doped material. Based on these observations, we have investigated the crystal structure and PL properties of the Eu^{3+} and Tb^{3+} activated $Na_3Gd(BO_3)_2$ borate and compared it with the isostructural $Na_3Y(BO_3)_2$ [11] which was previously found to exhibit PL properties when doped with Eu^{3+} [7]. We show that the Gd host lattice exhibits higher Eu^{3+} and Tb^{3+} emission intensities than the Y one, contrary to what was predicted, and that the Tb^{3+} emission is enhanced by the energy transfer from Gd^{3+} to Tb^{3+} compared to Y^{3+}. The better performances of the Gd-host lattice are explained by the crucial role of the structure, namely the local symmetry of the Gd site and the Gd–Gd distances shorter than the Y–Y distances.

2. Experimental

$Na_3Ln_{0.9}Eu_{0.1}(BO_3)_2$ (Ln=Y, Gd) and $Na_3Ln_{1-x}Tb_x(BO_3)_2$ (Ln=Y, Gd; x=0.07, 0.1, 0.2, 0.4, 0.6, 0.8, 1.0) phases were prepared by solid state reaction as reported in the literature [7]. The starting materials used were Na_2CO_3 (99.8%, Alfa Aesar), H_3BO_3 (99.9%, Alfa Aesar), Y_2O_3, Gd_2O_3, Tb_4O_7 and Eu_2O_3 (99.9%, Alfa Aesar). Y_2O_3, Gd_2O_3, Tb_4O_7 and Eu_2O_3 were preheated separately at 900 °C overnight for purification and to decompose Tb_4O_7 into Tb_7O_{12} [12]. Then the stoichiometric precursors were weighed accurately and were mixed together using an agate mortar and pestle. During grinding, a small amount of ethanol was added in order to mix the precursors homogeneously. The well ground precursors were placed in a platinum crucible and heated at 900 °C for 24 h with one intermittent grinding. The compounds were finally quenched to room temperature in air.

The phase purity of the above samples was analyzed using a Panalytical X'pert Pro X-ray diffractometer with a CuK_α source (λ=1.5418 Å). For the structural study the X-ray Powder Diffraction

* Corresponding author.
E-mail address: sophie.boudin@ensicaen.fr (S. Boudin).

0022-4596/$ - see front matter © 2012 Elsevier Inc. All rights reserved.
doi:10.1016/j.jssc.2012.02.042

(XRPD) pattern was registered for $2\theta=5^\circ$ to 120° with steps of 0.013° using also a Panalytical X'pert Pro X-ray diffractometer with a CuK_α source ($\lambda=1.5418$ Å). The crystal structure of the parent $Na_3Gd(BO_3)_2$ phase was refined by Rietveld method using the Fullprof program [13]. Diffuse reflectance spectra were measured by using a CARY 100 Varian spectrophotometer over the spectral range of 200–800 nm. PTFE was used as a reference for 100% reflectance. Excitation and emission spectra were recorded every 1 nm by using a Fluorolog-3 Horiba Jobin Yvon spectrophotometer having a 450 W Xenon lamp. All measurements have been carried out at room temperature.

3. Results and discussion

For the above experimental conditions pure phases were obtained for the borates $Na_3Ln_{0.9}Eu_{0.1}(BO_3)_2$ and $Na_3Ln_{1-x}Tb_x(BO_3)_2$ with Ln=Y, Gd and $x=0.07$, 0.1, 0.2, 0.4, 0.5, 0.6 and 0.8). The XRPD patterns of the undoped phase $Na_3Gd(BO_3)_2$ (Fig. 1) confirms its isotypism with the borates $Na_3Y(BO_3)_2$ [11] and $Na_3Nd(BO_3)_2$ [14]. Thus, its cell parameters were refined in the same monoclinic cell (space group $P21/c$) (Table 1), but it can be seen that the three crystal lattices exhibit significantly different distortions.

3.1. Crystal structure of $Na_3Gd(BO_3)_2$

The atomic parameters obtained from structural refinement for $Na_3Gd(BO_3)_2$ (Table 2) show that the atoms of this borate are considerably shifted with respect to $Na_3Y(BO_3)_2$, in spite of the isotypism of the two phases. The comparison of the interatomic distances and angles of these two borates (Table 3) clearly shows

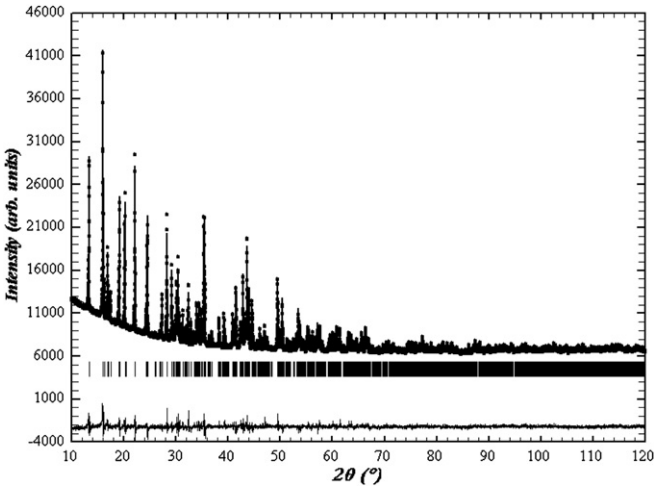

Fig. 1. X-ray powder diffraction patterns of $Na_3Gd(BO_3)_2$ (observed, calculated and difference patterns are represented with dots, bold line and solid line, respectively; positions of Bragg reflections with vertical bars).

Table 1
Lattice parameters for $Na_3Ln(BO_3)_2$ (Ln=Y, Gd, Nd).

	Ln=Y [11]	Ln=Gd (this work)	Ln=Nd [13]
Space group	$P2_1/c$ (no.14)	$P2_1/c$ (no. 14)	$P2_1/c$ (no. 14)
a (Å)	6.5050(3)	6.52297(6)	6.618(5)
b (Å)	8.5172(1)	8.72831(8)	8.810(5)
c (Å)	12.0213(1)	12.1476(1)	12.113(5)
β (°)	118.73(7)	123.3525(5)	122.27
Cell volume (Å^3)	584.04(2)	577.712(9)	597.12

Table 2
Atomic parameters and agreement factors of $Na_3Gd(BO_3)_2$.

Atom	Wyckoff position	x	Y	Z	Biso (Å^2)	Site occupation (%)
Gd	4e	0.1948(3)	0.1139(2)	0.3530(2)	0.5*	100
Na1	4e	0.367(2)	0.729(1)	0.3504(9)	2.0(2)	100
Na2	4e	0.120(2)	0.3170(9)	0.1006(8)	2.0(2)	100
Na3	4e	0.313(2)	0.9425(9)	0.0996(8)	2.0(2)	100
B1	4e	0.118(4)	0.419(3)	0.355(2)	0.7*	100
B2	4e	0.369(4)	0.595(3)	0.134(2)	0.7*	100
O1	4e	0.288(2)	0.347(2)	0.470(1)	0.7(1)	100
O2	4e	0.030(2)	0.364(2)	0.236(1)	0.7(1)	100
O3	4e	0.088(2)	0.562(1)	0.384(1)	0.7(1)	100
O4	4e	0.167(2)	0.604(2)	0.147(1)	0.7(1)	100
O5	4e	0.562(2)	0.025(1)	0.409(1)	0.7(1)	100
O6	4e	0.514(2)	0.711(1)	0.193(1)	0.7(1)	100

$R_{Bragg}=10.7\%$, $R_f=9.73\%$, $R_p=1.58\%$, $R_{wp}=2.26\%$, $R_{exp}=1.13\%$.
* fixed parameters.

that if the geometry of the BO_3 groups is very similar, it is not the case of the coordination of the lanthanide and sodium ions, which is strongly different. In particular, in $Na_3Y(BO_3)_2$, the Y^{3+} cation exhibits a seven fold coordination characterized by the pentagonal bipyramids YO_7, with Y–O distances ranging from 2.142(8) Å to 2.413(1) Å, whereas in $Na_3Gd(BO_3)_2$, one observes monocapped pentagonal bipyramids GdO_8 (Fig. 2), implying for Gd^{3+} and eight fold coordination with Gd–O distances ranging from 2.36(1) Å to 2.58(2) Å. As a consequence, the connection between the YO_7 bipyramids is significantly different from that between the GdO_8 monocapped bipyramids as shown from Fig. 3. The projection of the structure of $Na_3Y(BO_3)_2$ along b direction (Fig. 3(a)) shows that the YO_7 bipyramids form isolated chains running along b direction. Within the chains the YO_7 polyhedra share corners. The $B(1)O_3$ triangles complete the connection between the YO_7 polyhedra within the chains and the $B(2)O_3$ triangles ensure the connection between the chains. In contrast, in $Na_3Gd(BO_3)_2$ (Fig. 3(b)), successive chains of GdO_8 polyhedra (directed along b) have been brought closer to each other, along the $a+c$ direction, so that an oxygen atom (O5) of one GdO_8 polyhedron of one chain has been additionally linked to one GdO_8 polyhedron of the next chain. As a result, each Gd^{3+} ion reaches a eight fold GdO_8 coordination and two closed GdO_8 polyhedra share one edge. The GdO_8 polyhedron exhibits a monocapped pentagonal bipyramidal environment. Each GdO_8 polyhedron shares one edge with an other GdO_8 polyhedron in the (a,c) plane and two apices with two adjacent GdO_8 polyhedra along b, forming layers of edge and corner shared GdO_8 polyhedra parallel to $(\bar{1}\,0\,1)$. The $B(1)O_3$ triangles complete the connection between the GdO_8 polyhedra within the layers and the $B(2)O_3$ triangles ensure the connection between the layers. (Fig. 3(b)). This different mode of linking of the YO_7 and GdO_8 polyhedra makes that the Y–Y and Gd–Gd distances are very different in the two structures. One indeed observes Y–Y distances of 4.590(1) Å along the chains in $Na_3Y(BO_3)_2$, whereas the Gd–Gd distances are of 4.977(2) Å along the same b direction for $Na_3Gd(BO_3)_2$. But, more importantly, the latter phase exhibits much shorter distances of 4.114(2) Å between the edge sharing groups. Clearly, one can expect that the significantly different geometry of the $[GdO_6]_\infty$ framework compared to the $[YO_6]_\infty$ one will have a great impact upon their luminescence properties.

3.2. Diffuse reflectance spectroscopy

The diffuse reflectance spectra of the parent compounds were shown in the Fig. 4. Optical absorption edges are observed at 210 and 256 nm for $Na_3Y(BO_3)_2$ and $Na_3Gd(BO_3)_2$, respectively. In the